metals

MDPI

Article

Kinetic Investigation of Silver Recycling by Leaching from Mechanical Pre-Treated Oxygen-Depolarized Cathodes Containing PTFE and Nickel

Jil Schosseler [1,*], Anna Trentmann [1], Bernd Friedrich [1], Klaus Hahn [2] and Hermann Wotruba [2]

[1] Institute of Process Metallurgy and Metal Recycling IME, RWTH Aachen University, Intzestraße 3, 52056 Aachen, Germany; atrentmann@metallurgie.rwth-aachen.de (A.T.); bfriedrich@metallurgie.rwth-aachen.de (B.F.)

[2] Unit of Mineral Processing AMR, RWTH Aachen University, Lochnerstraße 4-20 Haus C, 52064 Aachen, Germany; hahn@amr.rwth-aachen.de (K.H.); wotruba@amr.rwth-aachen.de (H.W.)

* Correspondence: jschosseler@metallurgie.rwth-aachen.de; Tel.: +49-241-80-90855

Received: 26 November 2018; Accepted: 31 January 2019; Published: 5 February 2019

Abstract: This paper focuses on the recycling of silver from spent oxygen-depolarized cathodes through an innovative combination of pre-treatment methods and leaching. A silver- and polytetrafluorethylene (PTFE)-rich fraction was produced by cryogenic milling, screening, and magnetic separation. In order to understand the kinetic leaching mechanism, the silver-rich fraction was leached by different concentrations of nitric acid and hydrogen peroxide. Results showed that nickel influences the silver leaching. This leads to complex reaction systems, which cannot be described by the Arrhenius law.

Keywords: oxygen-depolarized cathodes; silver leaching; cryogenic pre-treatment; negative activation energy

1. Introduction

The utilization of oxygen-depolarized cathodes (ODCs) for chlorine-alkaline electrolysis is becoming interesting as an industrial process due to its lower energy consumption and associated CO_2 emission compared to mercury, diaphragm, or conventional membrane cell electrolysis [1]. The power consumption for chlorine production can be reduced to 30% compared to that of the common membrane process [2].

Oxygen-depolarized cathodes consist of a grid material made of nickel, silver powder as a catalyst, and polytetrafluorethylene (PTFE). As the technology becomes more relevant in the future, the development of a recycling process for used cathodes is an important step towards a sustainable process chain. This publication focuses on the recovery of silver from ODCs with a combination of mechanical pre-treatment and hydrometallurgical methods. The main objective is to extract the silver from the ODC as silver nitrate and produce an optimal silver nitrate solution that is suitable for subsequent silver electrolysis. The main challenge is to leach with a relatively low acid concentration, so that electrolysis can run at pH values of 5–6 without requiring strong neutralization. Furthermore, the nickel concentration in the electrolyte has to be below 1 g/L as nickel influences the silver powder morphology and its quality for reuse in ODCs. The influence of nickel in the silver electrolysis was investigated by a project partner and is not a part of this paper [3].

To develop a zero-waste recycling process for used oxygen-depolarized cathodes, the combination of mechanical pre-treatment and leaching was necessary for the following reasons:

- Pyrometallurgical treatment is not suitable because of the complex material composition and the high amount of PTFE. The combustion of PTFE produces harmful off-gases and requires a

complex off-gas cleaning [4]. Furthermore, a pyrometallurgical separation of silver and nickel causes high silver losses, which are investigated in other trials.

- The direct leaching of non-pre-treated oxygen-depolarized cathodes is technically feasible but requires a complex separation of dissolved nickel in order to recover catalytically active silver powder via silver electrolysis. Single pre-trials (5% nitric acid) with non-pre-treated cathodes revealed a higher dissolved nickel content (8 g/L Ni) compared to pre-treated ODCs (0.08 g/L Ni). For this reason, further experiments were carried out with crushed cathodes.
- The mechanical pre-treatment of the ODCs leads to the liberation of the enclosed silver particles, which improves the contact of acid and silver. A visual analysis of the pre-treated material showed a significant exposure of silver particles. In addition, handling crushed material is much easier compared to dealing with complete cathodes.
- Due to the relatively low acid concentration required, the influence of an oxidizing agent (hydrogen peroxide) and its influence on leaching (thermal instability [5] and catalytic decomposition [6]) should be investigated.

A zero-waste process is possible because the pre-processing of ODCs separates magnetic nickel, which can be melted directly after one washing step. Silver will be regained as silver powder for new ODCs from the obtained silver nitrate solution after leaching. Due to its chemically inert behavior, a PTFE fraction is received after leaching and filtration. After an additional leaching with concentrated acid, the PTFE should theoretically be clean enough to be transferred to a new recycling process.

The schematic of the developed recycling procedure, which should be able to deal with the challenges presented, is shown in Figure 1. The mechanical treatment started with cryogenic grinding in a cutting mill under liquid nitrogen. Temperatures below −50 °C increased embrittlement and supported the comminution of the material in the mill, which was necessary for the following processing steps. Separation was achieved by screening and magnetic separation, producing both an enriched Ni and a PTFE–Ag fraction. The enriched PTFE–Ag fraction was the input material for the following leaching step with nitric acid. The silver nitrate solution after leaching was used to produce silver powder by electrolysis, which, however, is not a part of this publication.

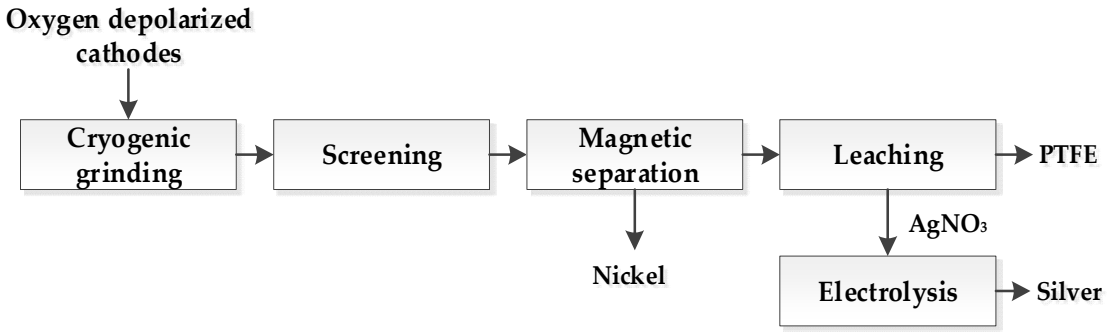

Figure 1. Schematic procedure for recycling silver from oxygen-depolarized cathodes (ODCs).

As shown in the flow sheet for the developed recycling process, the main objective was to devise a pre-treatment for used ODCs and to specify leaching conditions to obtain a suitable $AgNO_3$ solution for subsequent silver electrolysis.

The mechanical processing of the material uses mechanisms that are already well established in the processing of several mineral resources. Whereas screening is normally used to achieve a defined feed grain size for the subsequent separation processes, it can also be used to separate materials with different shapes in combination with selective comminution. There have been various approaches to selective comminution and subsequent screening for materials, such as concrete and mineral construction and demolition wastes in order to recycle their different components [7,8].

Magnetic separation has been increasingly used since the beginning of the 20th century. Its most important field of application is iron ore processing, as strong magnetic magnetite is enriched almost exclusively in this way. Due to its high susceptibility, metallic nickel is characterized as a ferromagnetic material that behaves similarly to magnetite, whereas Ag–PTFE is non-magnetic. This

makes the application of a dry low-intensity magnetic separation (LIMS) suitable for the investigated material [9]. Modern dry LIMS aggregates are mainly designed as drum separators with permanent magnets, providing magnetic field strengths below 2000 Gauss (0.2 Tesla) [10]. For small-scale applications, rotary magnetic belt separators with higher magnetic field strengths (up to 5000 Gauss) can be applied.

Silver leaching with nitric acid is a well-known procedure with a complex reaction between metal and acid with a dependency on purity, formed reaction products, and temperature. The chemical and physical state of silver also influences the reaction [11]. Furthermore, the acid concentration can change the reaction order. In a concentration range between 3.0 and 4.9 mol/L, the reaction follows the second order [12]:

$$4HNO_3 + 3Ag \longrightarrow 3AgNO_3 + NO + 2H_2O; \quad (1)$$

at higher acid concentrations (4.9–7.1 mol/L) silver reacts with nitric acid according to the first order [12]:

$$2HNO_3 + Ag \longrightarrow AgNO_3 + NO_2 + H_2O. \quad (2)$$

Also, the reaction system presented in this paper had to be extended because of the partially enclosed silver particles in a PTFE matrix, which certainly influenced diffusion.

A non-catalytic heterogeneous solid–fluid reaction of uniform spherical particles can be expressed with the shrinking core model. Here, the rate-controlling step can be expressed differently under two different scenarios. If the chemical reaction is the dominant step, the expression can be indicated as [13]:

$$1-\left(1-\alpha\right)^{1/3} = k \cdot t\,, \quad (3)$$

where α is the conversion, k is the reaction rate constant, and t is time.

If the diffusion of the reagent through a solid porous layer dominates the reaction, then the shrinking core model can be expressed, e.g., by an equation proposed by Jander [14]:

$$\left(\left(1+\alpha\right)^{1/3} - 1\right)^2 = k \cdot t\,. \quad (4)$$

A plot of $[1 - (1 - \alpha)^{1/3}]$ with respect to $[((1 + \alpha)^{1/3} - 1)^2]$ versus time should give a straight line with a slope k. Furthermore, the reaction rate constant is a function of temperature and the activation energy of the system can be determined by the Arrhenius equation (Equation 5) [15]:

$$k = Ae^{-E_a/RT}, \quad (5)$$

where A is the pre-exponential factor, E_a the activation energy, R the gas constant, and T the temperature.

The Arrhenius equation is applicable for elementary reactions between reactants, which are in an endothermic equilibrium. Furthermore, the reaction pathway from the initial to the final state does not influence the activation energy. The Arrhenius law suggests that the activation energy is a constant, which is not always a given, as E_a can show temperature and reaction-phase dependence [16,17].

2. Materials and Methods

To provide a sufficient liberation of the main components, the material was crushed by a cutting mill under cryogenic conditions. The low temperature of liquid nitrogen led to the embrittlement of the PTFE and nickel grid. Thus, a slight comminution of ODCs was possible without major material loss. A rough separation was seen after treatment (Figure 2a). The nickel grid matrix was disassembled into threads and the PTFE with the silver into grains (Figures 2b, c). The grain size was controlled by using different discharge screens (mesh sizes: 1, 2, and 4 mm). Five different batches were generated, whereby the first two batches (fractions 1 and 2) were used to generate enough

material for the leaching trials with a discharge screen of 4 mm. In order to investigate the liberation grade, three fractions were generated with different discharge screens. The influence of using different mesh sizes during cryogenic milling on chemical composition, grain size distribution, and leaching behavior was investigated separately. The different fractions obtained underwent the same processing steps afterwards.

Figure 2. Samples after cryogenic treatment. (**a**) Macroscopic image, (**b**) microscopic image of the nickel fraction, and (**c**) microscopic image of the Ag–polytetrafluorethylene (PTFE) fraction.

The main objective of mechanical processing was to generate a high-grade Ag–PTFE concentrate by rejecting the metallic Ni threads. This was achieved by dry magnetic separation. Due to the fact that the Ni threads tended to stick together and agglomerate with Ag–PTFE, the feed had to be deagglomerated by short-time screening. As a positive side effect, the screening process not only ensured deagglomeration but also separated an adequate amount of Ni threads. A simplified flow sheet of the discontinuous process is shown in Figure 3.

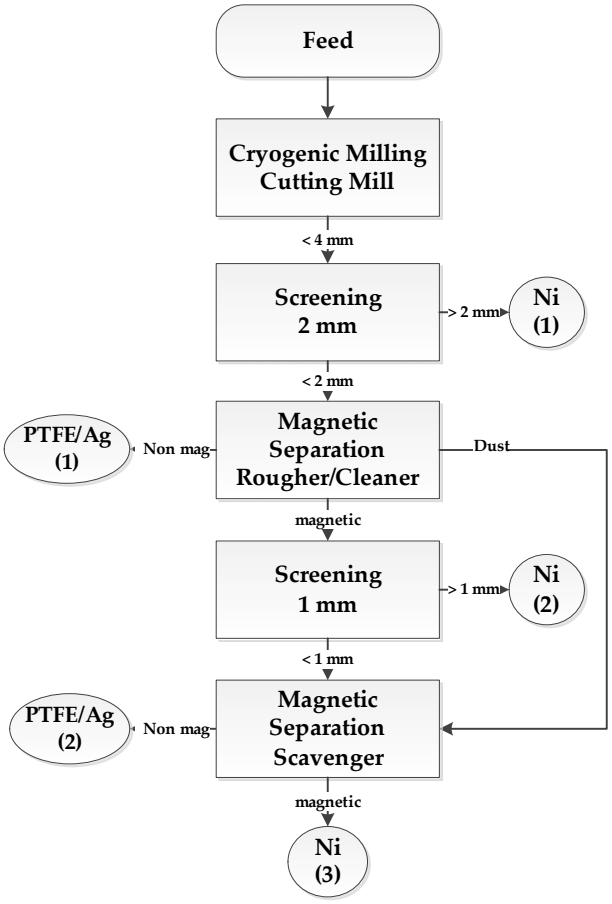

Figure 3. Simplified flow sheet of the discontinuous mechanical treatment process.

Screening was carried out using a laboratory-scale sieve, whereas magnetic separation was carried out with a rotary magnetic belt separator (Steinert, Cologne, Germany) with a permanent magnetic strength of 3500 Gauss (0.35 Tesla). To ensure a clean Ag–PTFE product and to speed up the recovery, a two-staged magnetic separation was performed followed by another short-time screening and a subsequent magnetic separation step.

The analysis of the processed ODCs was conducted with inductively coupled plasma atomic emission spectroscopy (ICP-AES) (Spectro Ciros Vision, Spectro, Kleve, Germany) after a microwave digestion (Multiwave PRO, Anton Paar, Graz, Austria) in concentrated nitric acid. By back weighing, the amount of insoluble PTFE was determined.

Leaching trials of the processed ODCs were carried out in a magnetic stirred beaker with a stirring speed of 300 rpm. To minimize fluid loss during the experiment, a watch glass was placed on the opening of the beaker. The solid to liquid ratio (50 g/L) and the temperature of 50 ± 1 °C was constant for all the leaching experiments. A reaction volume of 0.750 L was chosen and the material was homogenized for every trial to reduce the influence of material inhomogeneity.

In the first step, two different nitric acid concentrations were tested (5% HNO_3 and 10% HNO_3). Further, the influence of the addition of hydrogen peroxide was investigated. For this purpose, the required amount of H_2O_2 was calculated from the silver content and 1:1.5 and 1:3 Ag:H_2O_2 stoichiometries were chosen. The overstiochiometrical addition was chosen because a loss of hydrogen peroxide was anticipated due to thermal decomposition and reaction with nickel. At 120 min and at 240 min a liquid sample of 10 mL was taken and filtered with a syringe filter unit (mesh size 0.45 μm). The trials were repeated three times to prove the reproducibility and to reduce the influence of inhomogeneity of the material.

For the kinetic trials a temperature range from room temperature to 85 ± 0.5 °C was chosen. Over a time frame of 240 min, every 30 min a small sample of 10 mL was taken and filtered with syringe filter units (mesh size 0.45 μm). The agitation speed and the solid to liquid ratio were adopted from the leaching tests. The experiments were carried out with 5% nitric acid and a 1:3 stoichiometry was chosen to investigate the influence of hydrogen peroxide. The acid concentration of 5% and 1:3 stoichiometry delivered good results for the required selectivity and silver recovery for a possible recycling process. The results of the kinetic study provided information about the activation energy as well as details about the temperature and diffusion behavior in order to refine leaching parameters. The kinetic trials were repeated two times.

The silver concentration was determined with titration against chloride and nickel using ICP analysis. The liquid loss due to sampling and evaporation was taken into account for the calculation of the mean yields.

3. Results and Discussion

The results of five different test samples are shown in Table 1. Coarse- and medium-grained samples showed similar behavior in the first magnetic separation stage, while the recovery of Ag–PTFE from the fine-grained sample was less effective. The second magnetic separation stage increased the mass recovery of Ag–PTFE in all five samples.

As mentioned above, the process was not designed continuously because of the short-time screening stages between the milling and the magnetic separation stages. To realize an industrial and dry continuous process with a higher throughput, the application of an air jig or air tables could be considered due to the higher density of the Ag-bearing PTFE material compared to the Ni threads [18].

Table 1. Mass recoveries of mechanical processing tests.

Fraction	1 (Coarse)	2 (Coarse)	3 (Coarse)	4 (Middle)	5 (Fine)
Ni > 2 mm (1)	7.8%	8.4%	6.9%	8.2%	5.3%
PTFE–Ag magnetic separation rougher/cleaner (1)	73.2%	70.2%	74.7%	72.5%	61.2%
Ni > 1 mm (2)	8.4%	8.5%	8.5%	6.7%	11.3%
PTFE–Ag magnetic separation scavenger (2)	5.5%	10.6%	7.8%	7.5%	13.2%
Ni magnetic separation scavenger (3)	5.1%	2.3%	2.2%	5.1%	9.0%
Ag–PTFE product	78.8%	80.8%	82.4%	80.0%	74.4%
Ni fraction	21.2%	19.2%	17.6%	20.0%	25.6%

For the following leaching trials the non-magnetic fractions of 1 and 2 were taken and homogenized. Table 2 shows the material composition of the obtained Ag–PTFE fraction.

Table 2. Composition of processed ODCs used for leaching trials.

Ag	Ni	PTFE
91%	0.25%	5.7%

Figure 4 shows the metal extraction for silver and nickel after leaching with 5% and 10% HNO_3 and the addition of different amounts of hydrogen peroxide. By leaching with 5% nitric acid the silver yield reached 63.9% after 120 min; after 240 min the metal extraction increased to 85.2% (Figure 4a). The addition of hydrogen peroxide improved the silver recovery, as the yield reached 83.6% with 1:1.5 or 93.1% with 1:3 stoichiometry. A longer reaction time resulted in a slight increase up to 98.7% (1:3 stoichiometry). The silver dissolution reaction took place at the very beginning and almost reached a steady state after 120 min with the addition of hydrogen peroxide. For the extraction of nickel, a yield of 66.9% was obtained with the lower acid concentration after 120 min. The addition of the oxidizing agent decreased the nickel recovery to 47.1% with 1:3 stoichiometry. Similar to the dissolution of silver, the nickel dissolution also reached a saturation value after 120 min.

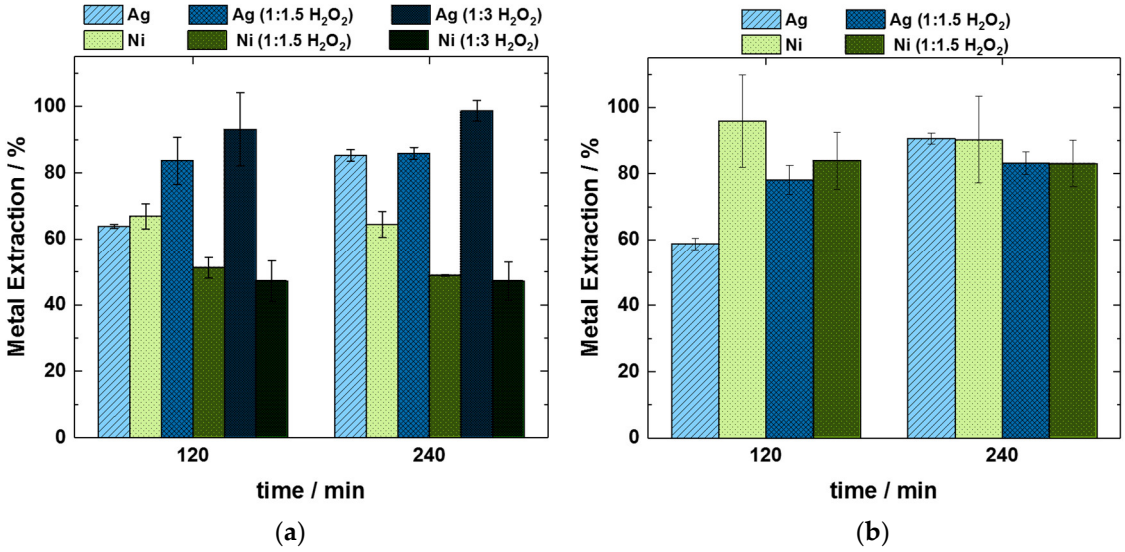

Figure 4. Recovery rate for silver and nickel for leaching trials with (**a**) 5% HNO_3 and (**b**) 10% HNO_3.

By leaching with 10% nitric acid, a slightly lower silver yield of 58.7% was obtained compared to the leaching trials with 5% HNO_3 (Figure 4b). The addition of hydrogen peroxide increased the silver recovery to 78.1%. A higher acid concentration led to a higher amount of nickel in the solution compared to leaching trials with 5% HNO_3. Additionally, the influence of the oxidizing reagent was significantly smaller and resulted in a lower silver-to-nickel selectivity. The lower acid concentration was more suitable for producing a silver nitrate solution ideal for electrolysis. Furthermore, the

addition of hydrogen peroxide decreased the dissolved nickel content and reduced the reaction time, as shown in Figure 4.

A recovery of 100% was not achieved due to the following observations: Some silver particles were partly or completely surrounded by the PTFE matrix. Consequently, direct contact between the nitric acid and the silver particles was impeded. Furthermore, the presence of metallic nickel threads led to the cementation of metallic silver on the nickel surface. Through this cementation reaction, nickel was passivated as soon as sufficient silver dissolved to cover the nickel surface. This reaction between the dissolved silver and metallic nickel grains results in a useful nickel saturation because of a desired low nickel concentration in the solution on the one hand but consequently leads to silver losses on the other hand.

The influence of different temperatures is shown in Figure 5. The dissolution of silver in 5% HNO_3 at room temperature was slower compared to that at higher temperatures. At room temperature, a delay in the dissolution of silver can be observed for less than 60 min. Due to previous experiences it can be assumed that silver dissolution is dominated by the silver cementation.

At 45 °C, the yield of silver reached a maximum at 80.6%. Higher temperature increases led to reduced silver extraction. The dissolution of silver with the H_2O_2 additive was significantly faster than without it. This can be attributed to the higher standard potential of H_2O_2 compared to that of HNO_3, meaning that silver oxidation occurred more easily. The temperature behavior of the HNO_3–H_2O_2 leaching curves was similar to the HNO_3 curves. The yield increased from 88.0% to 93.7% with a temperature rise of 15 °C after 60 min. However, a further increase in temperature led to lower silver yields.

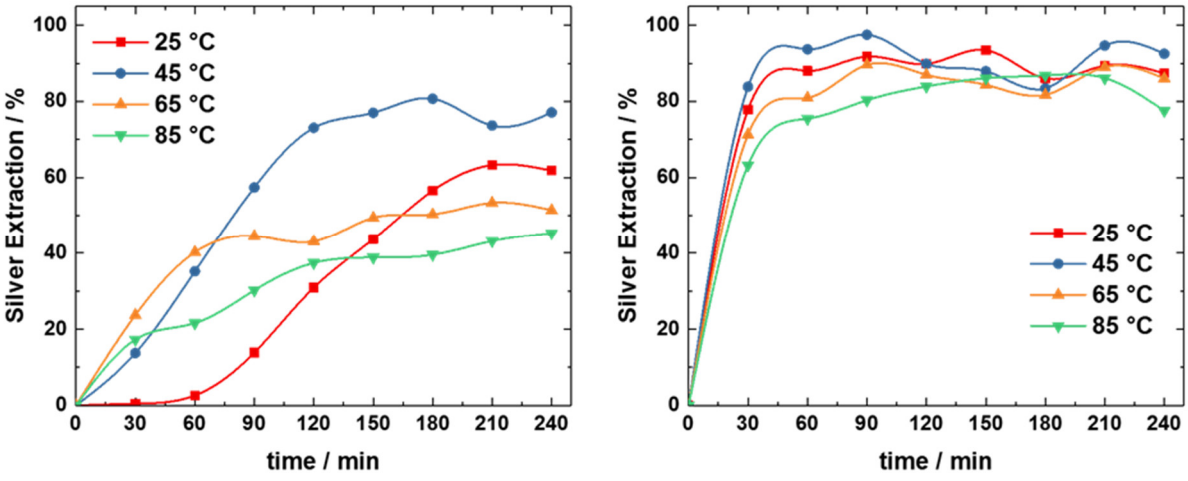

Figure 5. Silver extraction at different temperatures (**a**) without and (**b**) with the addition of hydrogen peroxide.

By applying the kinetic models stated above over a time range of 60–180 min, the following diagrams were created. The time range was chosen to exclude the range, where the silver extraction reached a saturation state. The differences between the models for reaction-controlled and diffusion-controlled leaching were only very marginal. Using other forms of the models also made no improvement. The main concern of the results obtained was the unusual behavior as a function of the temperature. The relationship between $1 - (1 - \alpha)^{1/3}$ (reaction-controlled) and $((1 + \alpha)^{1/3} - 1)^2$ (diffusion-controlled) and the time for silver leaching at various temperatures are shown in Figure 6. Comparing the two models, the quality of the linear regressions decreased with increasing temperature. In addition, based on the available data, no decision could be made as to whether the reaction is more diffusion- or reaction-controlled.

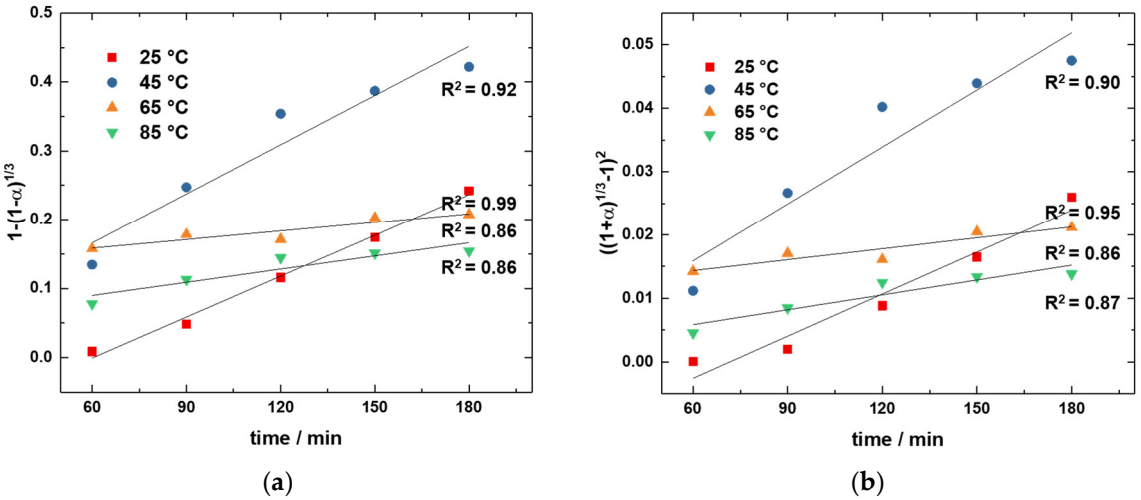

Figure 6. The relationship between (**a**) $1 - (1 - \alpha)^{1/3}$ (reaction-controlled) and (**b**) $((1 + \alpha)^{1/3} - 1)^2$ (diffusion-controlled) and the time for silver leaching at various temperatures.

After determining the reaction rate constants from the slopes, a decrease in the k values was observed with temperature increase. By plotting $\ln(k)$ versus $1/T$ in order to determine the activation energy following the Arrhenius equation, a negative activation energy was calculated for the dissolution of silver regardless of the chosen model. This outcome contradicts the literature values for the activation energy of metallic silver in nitric acid [12].

As mentioned in the introduction, the Arrhenius law depends on several factors [16,17]. Considering the observations of the reaction behavior, the non-Arrhenius behavior can be explained by the presence of a complex reaction system [19]. One assumption for the validity is a simple elementary reaction shown in Equation (6).

$$A + B \rightarrow C \quad (6)$$

One indication of the presence of a complex reaction is the leaching behavior of nickel. Leaching trials with 5% nitric acid have shown that it is impossible to achieve a complete dissolution of nickel in spite of its solubility in diluted nitric acid [20]. One possible explanation for this phenomenon is a passivation of the nickel threads after a certain reaction time and a subsequent hindrance for the dissolution of nickel. On examining the nickel threads after leaching by optical enlargement, a silver layer on the nickel surface was obvious from silver cementation (Figure 7).

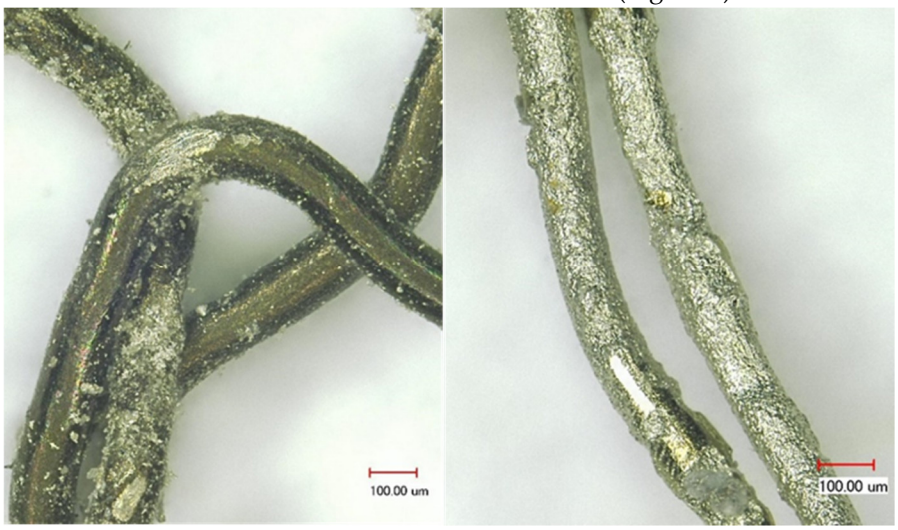

Figure 7. Silver cementation on nickel threads.

Considering this cementation, it was necessary to extend the model for the dissolution of silver with a consecutive reaction (Equation 7) which is a complex elementary reaction.

$$\left[\mathrm{Ag}\right]_{\mathrm{PTFE}} \xrightarrow{\mathrm{HNO_3}} \mathrm{Ag^+_{(aq)}} \underset{\mathrm{HNO_3}}{\overset{\mathrm{Ni}}{\rightleftharpoons}} \left[\mathrm{Ag}\right]_{\mathrm{Ni}}. \quad (7)$$

Furthermore, nickel shows a complex behavior, as it is dissolved in diluted acid and with silver cementation, which results in a parallel reaction.

$$\mathrm{Ni} \begin{cases} \xrightarrow{\mathrm{HNO_3}} \mathrm{Ni^{2+}_{(aq)}} \\ \xrightarrow{Ag^+} \mathrm{Ni^{2+}_{(aq)}} \end{cases} \quad (8)$$

Given the fact that both silver and nickel show complex dissolution reactions in this system, the requirements of the Arrhenius law are not fulfilled and the negative activation energy can be explained because of these phenomena. The three necessary reaction rate constants for the silver reaction include three different temperature dependences. Nickel dissolution can be expressed by two reaction rate constants. In addition, silver and nickel interact with each other, making the leaching model even more complicated. The overall reaction rate constant at one temperature, which is determined by the leaching model, is consequently a combination of several constants and depends on the concentration of the other metal, especially at the beginning of the reaction. By adding hydrogen peroxide, the reaction system will be extended at least for one reaction for each metal and even more reaction rate constants have to be considered. As a result, the kinetics of this system cannot be evaluated with the concepts of a shrinking core model and the Arrhenius law.

4. Conclusions

The kinetic investigation in the range of 25 °C to 85 °C led to a negative activation energy for the dissolution of silver. In the small temperature range from 25 °C to 45 °C, a positive activation energy was possible, but the data was insufficient to prove this. For higher leaching temperatures, a change in the leaching mechanism was possible, which was dominated by complex elementary reactions. In the future, further experiments should be conducted over smaller temperature and time ranges to determine a possible change in the reaction mechanism. The analysis of the data is difficult since little can be found in the literature about negative activation energy [21]. To work in the validity of the Arrhenius law, silver dissolution must be investigated without the influence of nickel. Due to the utilization of a recycled material, a pre-treatment was necessary.

For future kinetic investigations, it will be useful to study all possible chemical reactions. This is shown schematically in Figure 8 for the HNO_3–H_2O_2 system. The silver dissolution can occur on the one hand with nitric acid, where besides Ag^+ and water, nitrogen monoxide will also be formed. On the other hand, hydrogen peroxide can also react with silver to form Ag^+ and water. As the silver particles on the PTFE surface are in the micrometer range, H_2O_2 will decompose catalytically on the metal surface, leading to O_2 and H_2O formation and a slight temperature increase due to the exothermic reaction. Nickel can undergo reactions with nitric acid analogous to silver dissolution and with already dissolved silver to form nickel cations. Additionally, the oxidation of NO, which is formed by the metal–nitric acid reaction, to nitric acid should be mentioned as a side reaction.

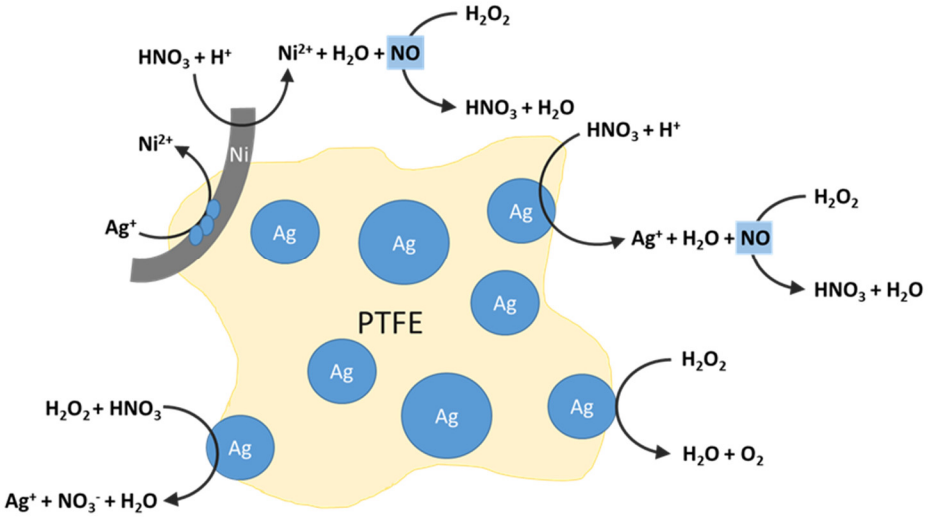

Figure 8. Schematic diagram for the possible reactions between silver, nitric acid, nickel, and hydrogen peroxide.

Author Contributions: Conceptualization and methodology: J.S., A.T., and K.H.; Writing—original draft preparation: J.S., A.T., and K.H.; Writing—review and editing: J.S., A.T., and K.H.; Supervision: B.F. and H.W.

Funding: The project upon which this publication is based was funded by the German Federal Ministry of Education and Research (BMBF) under Project Number 033R144.

Acknowledgments: Special thanks to Prof. Quicker and the Unit of Technologies of Fuels RWTH Aachen University, Germany for cryogenic milling and support. Another thanks goes to all project partners (Covestro Deutschland AG, Siegfried Jacob Metallwerke GmbH & Co KG, Department of Technical Thermodynamics RWTH University, and Institute for Non-Ferrous Metallurgy and Pure Materials TU Bergakademie Freiberg) for their support.

Conflicts of Interest: The authors declare no conflict of interest.

References

1. Sudoh, M.; Arai, K.; Izawa, Y.; Suzuki, T.; Uno, M.; Tanaka, M.; Hirao, K.; Nishiki, Y. Evaluation of Ag-based gas-diffusion electrode for two-compartment cell used in novel chlor-alkali membrane process. *Electrochim. Acta* **2011**, *56*, 10575–10581.
2. Jörrisen, J.; Turek, T. Chlorherstellung mit Sauerstoffverzehrkathoden. *Chem. Unserer Zeit Bd* **2011**, *45*, 172–182.
3. Schosseler, J.; Trentmann, A.; Alkan, G.; Friedrich, B.; Dressler, A.; Stelter, M.; Brück, S.; Dörner, H.; Bulan, A.; Douzinas, K.; et al. Silber-Recycling von Gasdiffusionselektroden aus der Chlor-Alkali-Elektrolyse. In *Berliner Recycling-und Rohstoffkonferent*; TK Verlag Karl Thomé-Kozmiensky: Neuruppin, Germany, **2018**; pp. 233–251.
4. Arito, H.; Soda, R. Pyrolysis products of polytetrafluoroethylene and polyfluoroethylenepropylene with reference to inhalation toxicity. *Ann. Occup. Hyg.* **1977**, *20*, 247–255.
5. Rice, F.O.; Reiff, O.M. The thermal decomposition of hydrogen peroxide. *J. Phys. Chem.* **1927**, *31*, 1352–1356.
6. Weiss, J. The catalytic decomposition of hydrogen peroxide on different metals. *Trans. Faraday Soc.* **1935**, *31*, 1547–1557.
7. Seifert, S.; Thome, V.; Karlstetter, C. Elektrodynamische Fragmentierung—Eine Technologie zur Effektiven Aufbereitung von Abfallströmen, Berliner Recycling-und Rohstoffkonferenz, TK Verlag Karl Thomé-Kozmiensky, Neuruppin, Germany, **2014**. Available online: http://www.vivis.de/phocadownload/Download/2014_rur/2014_RuR_431_438_Seifert.pdf (accessed on 20.12.2018).
8. Florea, M.V.A.; Ning, Z.; Brouwers, H.J.J. *Smart Crushing of Concrete and Activation of Liberated Concrete Fines*; University of Eindhoven, Department of the Built Environment, Unit Building Physics and Services: Eindhoven, The Netherlands, **2012**.

9. Schubert, H. *Aufbereitung Fester Mineralischer Rohstoffe, Band 2, 3*; Auflage, VEB: Leipzig, Germany, **1996**; pp. 125–172.
10. Mular, A.; Halbe, D.; Barratt, D. Mineral Processing Plant. *Des. Pract. Control* **2002**, *1*, 1069–1095.
11. Stansbie, J.H. The reaction of metals and alloys with nitric acid. *J. Soc. Chem. Ind.* **1913**, *XXXII*, 311–319.
12. Martinez, L.L.; Segarra, M. Kinetecs of the dissolution of pure silver and silver-gold alloys in nitric solution. *Metall. Trans. B* **1993**, *24B*, 827–835.
13. Levenspiel, O. *Chemical Reaction Engineering*, 2nd ed.; John Wiley & Sons, Int.: New York, NY, USA, **1972**; pp. 357–373.
14. Jander, W. Reactions in the Solid State at High Temperatures. *Z. Anorg. Allgem. Chem.* **1927**, *163*, 1–30.
15. Arrhenius, S. Über die Reaktionsgeschwindigkeit bei der Inversion von Rohrzucker durch Säuren. *Z. Phys. Chem.* **1889**, *4U*, 226–248.
16. Smith, I.W.M. The Temperature-dependence of elementary reactions rates: Beyond Arrhenius. *Chem. Soc. Rev.* **2008**, *37*, 812–826.
17. Vyazovkin, S. On the phenomenon of variable activation energy for condensed phase reactions. *New J. Chem.* **2000**, *24*, 913–917.
18. Wotruba, H.; Weitkämper, L.; Steinberg, M. *Development of a New Dry Density Separator for Fine-Grained Materials*; The Australian Institute of Mining and Metallurgy (XXV IMPC): Carlton, Australia, **2010**.
19. Muench, J.L.; Kruuv, J.; Lepock, J.R. A Two-Step Reversible-Irreversible Model Can Account for a Negative Activation Energy in an Arrhenius Plot. *Cyrobiology* **1996**, *33*, 253–259.
20. Holleman, A.F.; Wilberg, N.; Wilberg, E. *Anorganische Chemie, Band 2, 103*. Auflage, De Gruyter: Berlin, Germazy; Boston, MA, USA, **2016**; p. 2025.
21. McKibben, M.A.; Tallant, B.A.; del Angel, J.K. Kinetics of inorganic arsenopyrite oxidation in acidic aqueous solutions. *Appl. Geochem.* **2008**, *23*, 121–135.